CC Chemokine Receptor (CCR)2 Is Required for Langerhans Cell Migration and Localization of T Helper Cell Type 1 (Th1)-inducing Dendritic Cells: Absence of CCR2 Shifts the *Leishmania major*–resistant Phenotype to a Susceptible State Dominated by Th2 Cytokines, B Cell Outgrowth, and Sustained Neutrophilic Inflammation

By Naoko Sato,*‡ Sunil K. Ahuja,*‡ Marlon Quinones,*‡ Vannessa Kostecki,*‡ Robert L. Reddick,§ Peter C. Melby,*‡ William A. Kuziel,‖¶ and Seema S. Ahuja*‡

*From the *South Texas Veterans Health Care System, Audie L. Murphy Division, and the ‡Department of Medicine and the §Department of Pathology, University of Texas Health Science Center at San Antonio, San Antonio, Texas 78284-7880; and the ‖Section of Molecular Genetics and Microbiology and the ¶Institute of Cellular and Molecular Biology, University of Texas, Austin, Texas 78712-1095*

Abstract

There is growing evidence that chemokines and their receptors regulate the movement and interaction of antigen-presenting cells such as dendritic cells (DCs) and T cells. We tested the hypothesis that the CC chemokine receptor (CCR)2 and CCR5 and the chemokine macrophage inflammatory protein (MIP)-1α, a ligand for CCR5, influence DC migration and localization. We found that deficiency of CCR2 but not CCR5 or MIP-1α led to distinct defects in DC biology. Langerhans cell (skin DC) density in CCR2-null mice was normal, and their ability to migrate into the dermis was intact; however, their migration to the draining lymph nodes was markedly impaired. CCR2-null mice had lower numbers of DCs in the spleen, and this was primarily due to a reduction in the $CD8\alpha^+$ T helper cell type 1 (Th1)-inducing subset of DCs. Additionally, there was a block in the *Leishmania major* infection–induced relocalization of splenic DCs from the marginal zone to the T cell areas. We propose that these DC defects, in conjunction with increased expression of B lymphocyte chemoattractant, a B cell–specific chemokine, may collectively contribute to the striking B cell outgrowth and Th2 cytokine–biased nonhealing phenotype that we observed in CCR2-deficient mice infected with *L. major*. This disease phenotype in mice with an *L. major*–resistant genetic background but lacking CCR2 is strikingly reminiscent of that observed typically in mice with an *L. major*–susceptible genetic background. Thus, CCR2 is an important determinant of not only DC migration and localization but also the development of protective cell-mediated immune responses to *L. major*.

Key words: infectious immunity • chemokine • cytokine • knockout • T helper cell

Introduction

It is in the lymphoid organs that T lymphocytes and APCs such as B cells and dendritic cells (DCs)[1] participate to generate adaptive immune responses (1–4). The trafficking of these leukocytes is a tightly regulated multistep process.

---

[1]*Abbreviations used in this paper:* BLC, B lymphocyte chemoattractant; CCR, CC chemokine receptor; DC, dendritic cell; LC, Langerhans cell; MIP, macrophage inflammatory protein; MCP, monocyte chemoattractant protein; SLMA, soluble *Leishmania major* antigen; TUNEL, TdT-mediated dUTP nick end labeling.

However, the precise repertoire of signals that regulate these processes is not fully understood (1–8). Clearly, a better understanding of the determinants of leukocyte trafficking and cell–cell localization might offer new opportunities for therapeutic intervention to suppress or stimulate the immune response.

Recently, a central function for various chemokines and their receptors in lymphocyte and APC migration has been identified (3–8). Based on in vitro chemotaxis and chemokine receptor expression studies (5, 7, 9, 10) and the in vivo studies of Tang and Cyster (11), a model for the migration of DCs and Langerhans cells (LCs)—the skin counterparts of DCs—has been proposed (3, 4, 8). In this model, DC/LC migration is dependent on the selective responsiveness of immature and mature DCs/LCs to distinct sets of chemokines, as well as the chemokine-induced downregulation of the cognate chemokine receptor.

An important role for the chemokine system in DC/LC migration and maintenance of the microanatomic environment of secondary lymphoid organs has also emerged (3, 4, 12–18). Mice deficient in CC chemokine receptor (CCR)7 have impaired migration of lymphocytes and DCs and profound morphological alterations in the architecture of secondary lymphoid organs (13). A naturally occurring mouse strain with a mutation designated as paucity of lymph node T cells (*plt*) exhibits a defect in T cell homing, LC migration, and localization of DCs to the T cell zones of the spleen and lymph node (16). The genetic basis for the *plt* phenotype is thought to be due to a defect in the production of secondary lymphoid tissue chemokine (SLC) (16). Targeted inactivation of CXC chemokine receptor (CXCR)5 led to defects in the development of B cell follicles and in B cell migration, indicating a major role for CXCR5 and its ligand B lymphocyte chemoattractant (BLC) in mediating compartmental homing of B lymphocytes (12, 18).

In light of the emerging importance of various members of the chemokine system in DC biology, we tested the hypothesis that the chemokine receptors CCR2 and CCR5 and the chemokine macrophage inflammatory protein (MIP)-1α influence DC migration and localization. Understanding the function of this chemokine and these two receptors in DC biology and adaptive immune responses is of additional interest because they play an important role in HIV-1 pathogenesis (19). In contrast to mice deficient in CCR5 or MIP-1α, CCR2-null mice had significantly impaired LC migration, reduced numbers of CD11c+ splenic DCs (especially the Th1-inducing subset of DCs [20–22]), and a block in the *Leishmania major* infection–induced relocalization of splenic DCs from the marginal zone to the T cell areas.

In view of these findings, we used the cutaneous infection model of *L. major*, an intracellular parasite, to test the hypothesis that the broad range of DC/LC abnormalities in CCR2-deficient mice is associated with impaired adaptive immune responses. This model offers several unique advantages. First, *L. major*–infected LCs but not macrophages play a central role in initiating primary Ag-specific T cell responses (23, 24). This special function of LCs in experimental cutaneous leishmaniasis is especially helpful in differentiating the effects attributable to impaired LC migration versus the impaired monocyte migration observed in CCR2-null mice (25–28). Second, several lines of investigation have shown that susceptibility and resistance to *L. major* infection are associated with differential expansion of Th1 and Th2 cell subsets (29). For example, C57BL/6 mice develop a parasite-specific expansion of IFN-γ– and IL-2–producing Th1 cells and are able to control infection (healing phenotype). In contrast, BALB/c mice develop a dominant expansion of IL-4–, IL-5–, and IL-10–producing Th2 cells, marked B cell outgrowth (30, 31), sustained neutrophilic inflammation at the site of skin infection (32), and progressive disease (nonhealing phenotype).

Deficiency of CCR2 but not CCR5 or MIP-1α in an *L. major*–resistant genetic background led to a phenotype that was strikingly reminiscent of that observed in *L. major*–susceptible BALB/c mice. Interestingly, the CCR2-deficient mice appeared to be particularly primed for B cell expansion, because in both the uninfected and infected state they expressed significantly higher amounts of BLC, a B cell–specific chemokine (18). Taken together, these findings provide evidence for an important role for CCR2 in LC migration, expression of Th1-inducing DC subsets, infection-induced relocalization of DCs, and potentially B cell outgrowth. We propose that defects in these processes collectively contribute to the striking Th2-biased nonhealing phenotype observed in CCR2-deficient mice infected with *L. major*.

Materials and Methods

Mice and Parasites. The generation of CCR2$^{-/-}$, CCR5$^{-/-}$, and MIP-1α$^{-/-}$ mice has been described previously (28, 33, 34). Wild-type (+/+) and gene knockout mice were on an outbred C57BL/6J × 129/Ola genetic background ($n > 6$ generations). Mice were born and bred under specific pathogen-free conditions. At 5–6 wk of age, mice were transferred from the University of Texas at Austin to the University of Texas Health Science Center at San Antonio. The Institutional Animal Care and Use Committee approved all protocols. *L. major* clone VI (MHOM/IL/80/Friedlin) was a gift of Dr. D.L. Sack (National Institutes of Health, Bethesda, MD). The virulence of the *L. major* strain was maintained by propagating it in mice. Protocols similar to those used to prepare soluble *L. major* Ags (SLMAs) were used to make soluble *Leishmania donovani* Ags (35). The intradermal route was used to infect both ears with 2×10^6 stationary phase of *L. major* promastigotes resuspended in 20 μl PBS. A dial-thickness gauge caliper (Fred V. Fowler Co., Inc.) was used to measure ear thickness at weekly intervals for 5 wk. The organisms were grown in a biphasic medium containing blood agar (36), and the limiting dilution culture method was used to quantify parasite burden in the ears, draining lymph nodes, and spleens (37).

Materials. DMEM, RPMI 1640, medium 199, antibiotics, FCS, Hepes, PBS, and trypsin were obtained from Life Technologies. All chemicals were from Sigma-Aldrich and Abs were from BD PharMingen, unless otherwise stated.

Cells Migrating from Ear Skin Explants. The protocols used were those described by Larsen et al. (38) and Belkaid et al. (39,

40). In brief, the ears were dissected, rinsed in 70% ethanol with vigorous shaking, and allowed to dry for 15 min. The ventral and dorsal sheets were separated with a pair of fine forceps. The two leaflets were transferred dermal side down for 24 or 72 h in a 10-cm dish that contained culture medium (RPMI 1640 with 10% FCS and 25 mM Hepes). Cell populations that spontaneously emigrated out of the dermal layers were pooled. The loosely adherent cells were recovered by incubating the dermal layers in PBS containing 2 mg/ml glucose for 20 min at 37°C. The loosely adherent cells and spontaneously migrating cells were pooled together, filtered through a 70-μm nylon cell strainer, washed with PBS, and then stained. The LCs were identified as I-A^b bright and DEC-205$^+$. The neutrophils migrating from the skin explants were identified as cells that were Ly-6G bright and negative for I-A^b. CD4$^+$ T cells were identified as both CD3$^+$ and CD4$^+$. The localization of LCs in the epidermal sheets was analyzed as described by Gunn et al. (16). The migration of epidermal LCs into the dermal lymphatics was analyzed as described previously (41). In brief, after 72-h culture of ear explants, dermal sheets were fixed in acetone for 30 min, rehydrated in PBS, and incubated in 1:20 FITC-labeled anti–I-A^b mAb for 90 min at room temperature. After washing in PBS, the dermal sheets were mounted on microscope slides and evaluated by fluorescence microscopy.

Epidermis Cell Preparation. The methods and protocols were as described by Belkaid et al. (40). In brief, the ears were excised, rinsed in 70% ethanol with vigorous shaking, and left to dry for 15 min. The dorsal and ventral sheets were separated and placed in wells of 6-well plates containing 0.5% and 1% trypsin, respectively, for 30 min at 37°C. The epidermis was separated from the dermis and deposited on a 70-μm nylon cell strainer that was placed in wells of a 6-well plate containing DMEM with 20% FCS, 100 U/ml penicillin, 100 μg/ml streptomycin, and 0.05% DNase. The nylon cell strainer was shaken gently for 2 min, and the cells passing through were washed and incubated overnight at 37°C. Cells were stained with anti–DEC-205 mAb (NLDC-145; Serotec) followed by PE-labeled anti–rat Ig polyclonal Ab and FITC-labeled anti–I-A^b mAb, and were analyzed by FACSCalibur™ (Becton Dickinson).

LC Migration to Lymph Nodes. The protocols described (42–45) were used to track the migration of FITC$^+$ LCs from the skin to the draining lymph nodes. In brief, freshly prepared 5% FITC in 1:1 acetone/dibutylphthalate was painted on both sides of the ears (10 μl each) or on the abdomen (400 μl), and the draining lymph nodes were collected. For FACS® analysis, 24 h after the ears were painted with FITC, the draining lymph nodes were dissected, homogenized between the frosted ends of two microscope slides, filtered through a nylon mesh, treated with red blood cell lysing buffer, and washed with PBS. Cells were stained initially with anti–DEC-205 mAb and then biotin-labeled anti–rat IgG (Vector Laboratories). The cells were then stained with CyChrome 5–labeled streptavidin (Amersham Pharmacia Biotech) and PE-labeled anti–I-A^b mAb. Cells that were both FITC$^+$ and I-A^b bright were identified as LCs that had migrated from the ear into the draining lymph nodes. In additional experiments, after the abdomen was painted with FITC, the draining lymph nodes were harvested 6, 24, 48, or 72 h later and frozen in OCT compound (Sakura), and 5-μm cryostat sections were prepared. FITC$^+$ LCs in the sections of the draining lymph nodes were examined by fluorescence microscopy (Olympus).

In Vitro Ag Presentation Activity. For allogeneic mixed lymphocyte reactions, stimulator cells were metrizamide-enriched LC fractions harvested from the draining lymph nodes 24 h after the ears were painted with FITC. The metrizamide-enriched DCs/LCs (43) were treated with 60 μg/ml of mitomycin C (Calbiochem) for 30 min at 37°C. Responder cells were CD3$^+$ T cells purified from BALB/c spleens by a mouse T cell enrichment column (R&D Systems). Responder T cells (2 × 10^5) were incubated with varying concentrations of LCs for 96 h and pulsed with [^{3}H]thymidine (1 μCi/well; Amersham Pharmacia Biotech) during the last 18 h of culture. Cultures were then harvested on glass fiber filters (Skatron Instruments, Inc.) and counted by a β-scintillation counter. For Ag-specific syngeneic proliferation assays, DCs were purified from the spleen by the methods of Leenen et al. (46), then incubated with 200 μg/ml of KLH for 20 h at 37°C and treated with 60 μg/ml of mitomycin C. Preparation of Ag-primed lymph node T cells was as described previously (47). T cells (2 × 10^5) were incubated with varying concentrations of DCs for 4 d, and thymidine incorporation was determined.

Staining for DC Subtype in Spleen. Spleen cell suspensions were prepared by collagenase digestion (48) and washed with 5 mM EDTA-PBS. Cells were stained with FITC-labeled anti-CD8 mAb, PE-labeled anti-CD11c mAb, and allophycocyanin-labeled anti-CD11b mAb in the presence of anti-CD16/CD32 mAb (2.4G2) suspended in 5 mM EDTA-PBS.

Immunohistochemistry. Tissue samples of lymph nodes and spleens were frozen in OCT, and 5-μm cryostat sections were prepared. Sections were fixed in acetone for 10 min, air dried, blocked with 0.1% BSA in tris-buffered saline for 10 min, and incubated with unlabeled and biotin-labeled first mAb for 1 h. Slides were then washed in tris-buffered saline, incubated with horseradish peroxidase–labeled second Ab and streptavidin–alkaline phosphatase–labeled second Ab for 1 h, and developed with 3,3′-diaminobenzidine followed by Vector Blue or Vector Red (Vector Laboratories) according to the manufacturer's instructions. Similarly, double staining for apoptotic TdT-mediated dUTP nick end labeling (TUNEL)$^+$ cells was combined with anti-B220 mAb or anti-CD11c mAb according to the manufacturer's instructions (Boehringer). Each immunohistochemistry photomicrograph is representative of multiple lymph node or spleen sections derived from six to eight mice per group.

Histopathology. At necropsy, the ears were removed and placed in neutral buffered 10% formalin. After adequate fixation, the ears were embedded in paraffin. From each paraffin block, 5 μm–thick sections were cut and stained with hematoxylin and eosin. Each section was evaluated for the nature of the cellular infiltrate, organisms, and necrosis. The pathologist (R.L. Reddick) reviewing the histopathologic slides was blinded to the identity of the source of the tissue sections.

Ag-specific Cytokine and Ig Production. Ag-specific IL-4 and IFN-γ production from spleen or lymph node cells was determined. Single cell suspensions (5 × 10^6/ml) were cultured with or without 50 μg/ml of SLMA in 24-well plates. After 48 h of culture, supernatants were harvested, and ELISA was used to determine the cytokine levels. The methods for ELISA were as described previously (33). The useful ranges for ELISA were 2.0–125 pg/ml for IL-4, and 15.6-1,000 pg/ml for IFN-γ.

Measurement of Serum Ig by ELISA. SLMA (10 μg/ml) was coated onto 96-well plates. After blocking, serum from mice infected for 5 wk was added to the well, serially diluted, and incubated overnight at 4°C. After washing, wells were incubated with alkaline phosphatase–labeled anti–mouse Ig Ab, anti–mouse IgG1 mAb, anti–mouse IgG2a mAb, anti–mouse IgG3 mAb, or anti–mouse IgE mAb, washed, then developed and measured as described previously (33).

Northern Blot Analysis. Total RNA (20 μg) from lymph nodes of uninfected and infected wild-type and CCR2-null mice was subjected to gel electrophoresis, transferred to Hybond N[+] membranes (Amersham Pharmacia Biotech), and probed using randomly primed ^{32}P-labeled mouse cDNA probes. The following primers were used for making PCR-derived probes for BLC and glyceraldehyde 3-phosphate dehydrogenase (GAPDH): BLC, forward primer 5′-CAGGCAGAATGAGGCTCAG-3′ and reverse primer 5′-GGCAGCTCTTCTCTTACTCACTG-3′; and GAPDH, forward primer 5′-TTGAAGGGTGGAGC-CAAACG-3′ and reverse primer 5′-ACACATTGGGGGTAG-GAACACG-3′. For quantitation, films were scanned and analyzed by NIH Image software (v1.61). The BLC mRNA level was corrected for the amount of RNA loaded by dividing the BLC hybridization signal by the GAPDH signal.

Statistical Analysis. Results are expressed as mean ± SD. In instances where the data were not normally distributed, they were transformed into ranks and analyzed using analysis of variance to determine if there was an overall difference between the groups. Tukey's (see Fig. 5 and Fig. 6, A–H) or Dunnett's (uninfected mice; see Fig. 1 C, Fig. 6 I, and Table I) posthoc tests were used when an overall difference was observed. An unpaired two-tailed *t* test was used for between-group analysis (infected mice; see Fig. 8 D and Table I).

Results

Decreased Migration of LCs from Ear Skin Explants of CCR2- and CCR5-null Mice. The ear skin explant model (38, 40) and the model of FITC-induced LC migration (42–45) are the two well-characterized complementary approaches that we used to test the hypothesis that mice deficient in CCR2, CCR5, or MIP-α have impaired DC migration. The first model is an ex vivo model that allows for the examination of LC migration from the skin epidermis to the dermal lymphatics, whereas the latter model permits an in vivo analysis of LC migration to the draining lymph nodes. Previous studies have suggested that the migration of LCs out of ear skin explants into the culture medium in vitro may reflect, in part, their in vivo migratory capacity (38).

The cumulative number of DEC-205^{+}I-A[b+] (marker for LC/DC and MHC class II, respectively) cells that migrated out of the ear skin explants was greater at 72 h than at 24 h in +/+, CCR2$^{-/-}$, and CCR5$^{-/-}$ mice (Fig. 1 A). However, at both time points, the absolute number of LCs that emigrated from CCR2$^{-/-}$ skin explants was 66–99% lower than that of +/+ mice (Fig. 1, A and B). Compared with +/+ mice, the number of LCs that migrated from skin explants of CCR5$^{-/-}$ mice was also lower, but the defect was not as prominent as that seen in CCR2-null mice. In contrast to CCR2- or CCR5-null mice, the migration of LCs from the ear explants of MIP-1α–deficient mice was similar to that of +/+ mice (data not shown).

These findings suggested that CCR2-null mice might have a block in LC migration out of the dorsal ear skin. However, an alternative explanation could be that LC migration is normal, and that these findings are secondary to lower expression levels of DEC-205 in CCR2-null mice. In this situation, the proportion of DEC-205$^-$ but I-A[b+]
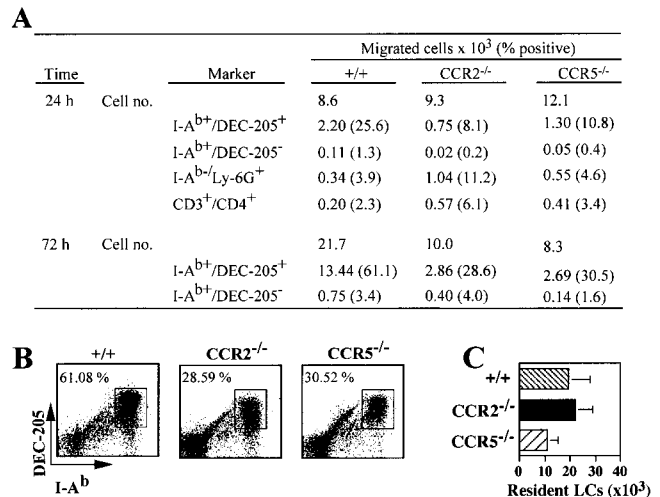
A

Time	Marker	Migrated cells x 10³ (% positive)		
		+/+	CCR2$^{-/-}$	CCR5$^{-/-}$
24 h Cell no.		8.6	9.3	12.1
	I-A[b+]/DEC-205^{+}	2.20 (25.6)	0.75 (8.1)	1.30 (10.8)
	I-A[b+]/DEC-205$^-$	0.11 (1.3)	0.02 (0.2)	0.05 (0.4)
	I-A[b-]/Ly-6G^{+}	0.34 (3.9)	1.04 (11.2)	0.55 (4.6)
	CD3^{+}/CD4^{+}	0.20 (2.3)	0.57 (6.1)	0.41 (3.4)
72 h Cell no.		21.7	10.0	8.3
	I-A[b+]/DEC-205^{+}	13.44 (61.1)	2.86 (28.6)	2.69 (30.5)
	I-A[b+]/DEC-205$^-$	0.75 (3.4)	0.40 (4.0)	0.14 (1.6)

Figure 1. Migration of LCs out of ear skin explants of CCR2$^{-/-}$ and CCR5$^{-/-}$ mice is reduced. (A) The absolute numbers of I-A[b+]DEC-205^{+} (LCs) and I-A[b+]DEC-205$^-$ cells emigrating out of ear skin explants was determined after 24 and 72 h of culture. The data for the 24- and 72-h time points are from one of two and one of three representative experiments, respectively. The migrating I-A[b-]Ly-6G^{+} (neutrophils) and CD3^{+}CD4^{+} (CD4^{+} T cells) cells were determined after 24 h of culture (one of three representative experiments is shown). Data from skin explants of three to seven mice per group were pooled for analysis. The percentages of I-A[b+]DEC-205^{+}, I-A[b+]DEC-205$^-$, I-A[b-]Ly-6G^{+}, and CD3^{+}CD4^{+} cells among the total number of cells that emigrated are shown in parentheses. (B) Representative FACS® profile showing a marked decrease in I-A[b+]DEC-205^{+} cells that migrated out of ear explants of CCR2$^{-/-}$ and CCR5$^{-/-}$ mice. (C) The I-A[b+]DEC-205^{+} cells (mean number ± SD) present in epidermal cell suspensions was determined by flow cytometry. Epidermal cell suspensions were prepared from three mice per group. Data are from one of two experiments with similar results.

cells should be higher in CCR2-null mice compared with +/+ mice. However, this was not the case. The I-A[b+]DEC-205$^-$ cells represented a small number of the migrating cells, and the knockout mice appeared to have similar or lower numbers of I-A[b+]DEC-205$^-$ cells compared with +/+ mice. The exact identity of the I-A[b+] but DEC-205$^-$ cells is not clear, but they may represent mast cells (39). In contrast to reduced numbers of LCs migrating out of the skin explants, the number of neutrophils migrating out was ~2–4-fold higher in CCR2-null mice compared with +/+ or CCR5-deficient mice (Fig. 1 A; data not shown). Compared with +/+ mice, the numbers of migrating CD4^{+} T cells was similar to (data not shown) or slightly higher (Fig. 1 A) in the CCR2-deficient mice.

Reduced LC migration in CCR2-deficient mice was not due to a lower density of resident epidermal LCs (Fig. 1 C), and by immunohistochemistry, the number and intraepidermal distribution of LCs also appeared normal in the different animal groups (data not shown). We excluded the possibility that the reduced LC migration was due to a block in the migration of LCs from the epidermis to the dermis by staining the epidermal sheets of the ear skin explants that had been in culture for 72 h. The epidermal layer in the skin explants of +/+, CCR2$^{-/-}$, and CCR5$^{-/-}$ mice contained only a few scattered I-A[b+] cells,

suggesting that most of these cells had moved into the dermis (data not shown).

As there were lower numbers of CCR2- and CCR5-deficient LCs migrating out, it would be expected that a disproportionately larger number of these LCs would be retained in the dermal layer. Indeed, this was the case. Compared with +/+ mice, the density of I-A^b–staining cells in the dermal ear skin that had been in culture for 72 h was greater in CCR2$^{-/-}$ and CCR5$^{-/-}$ mice (Fig. 2; data not shown). Migrating DCs typically form cords within the dermal lymphatics (38), and at higher magnifications, I-A^b cells appeared to be distributed in a pattern consistent with cords (Fig. 2). The cord formation was especially prominent in CCR2-deficient mice (Fig. 2 B). However, additional studies are required to clarify whether these I-A^b–staining cells distributed in the pattern of cords represent cells accumulated within the dermal lymphatics or those surrounding the lymphatics. Regardless of these two mechanistic possibilities, our findings suggest that mice deficient in CCR2 have a defect in LC migration that, at least in this ex vivo organ culture model of LC migration, is more significant than that found in CCR5-null mice.

Impaired FITC-induced LC Migration to Draining Lymph Nodes in CCR2-null Mice. We next used the well-established FITC-based contact hypersensitivity model to determine whether lack of expression of CCR2 influenced significantly the trafficking of LCs to the draining lymph nodes in vivo (42–45). Hill et al. (42) have shown previously that after painting of the skin with FITC, there is a rapid influx of FITC$^+$ LCs into the draining lymph nodes that peaks at 24 h; the levels of FITC-labeled DCs remain elevated for another 2 d, and then decline to normal levels by day 6.

We enumerated by fluorescence microscopy the number of lymph node sections bearing FITC$^+$ LCs at various time points after painting of the skin with FITC (Fig. 3, A–O, and data shown below). As early as 6 h after painting of the skin with FITC, FITC$^+$ LCs were found in ∼30% and ∼6% of the draining lymph nodes of +/+ (Fig. 3 A, and data shown below) and CCR5$^{-/-}$ mice (Fig. 3 C, and data shown below), respectively. These FITC$^+$ cells were localized primarily to the subcapsular region (Fig. 3, A and C). In contrast, at this time point, lymph nodes containing FITC$^+$ LCs were not found in the CCR2$^{-/-}$ mice (Fig. 3 B). By 24 h, ∼65% and ∼75% of lymph nodes from +/+ and CCR5$^{-/-}$ mice, respectively, contained FITC$^+$ LCs

(Fig. 3, D and F, and data shown below). In contrast, in CCR2$^{-/-}$ mice, the number of lymph node sections bearing FITC$^+$ LCs was substantially lower (∼22%; Fig. 3 E, and data shown below). In addition to this quantitative difference in the number of lymph node sections that contained FITC$^+$ LCs, there was a difference in the localization of these LCs. At 24 h after FITC painting, the FITC$^+$ LCs were dispersed throughout the lymph nodes of both +/+ (Fig. 3, D and G) and CCR5$^{-/-}$ mice (Fig. 3, F and I). However, in CCR2$^{-/-}$ mice, FITC$^+$ LCs could be detected only in or near the subcapsular region of the lymph nodes (Fig. 3, E and H). At 48 h, nearly 80–100% of lymph node sections from +/+ and CCR5$^{-/-}$ mice versus 50% of lymph node sections from CCR2$^{-/-}$ mice contained FITC$^+$ LCs. However, by 72 h, there was no difference in either the number or the localization of FITC$^+$ cells in any of the groups of mice.

The finding of reduced LC migration in CCR2-null mice was substantiated by flow cytometry analysis (Fig. 4). The number of I-A^{b+}DEC-205$^+$, CD11c$^+$CD8α$^+$, or CD11c$^+$CD11b$^+$ cells in non–FITC-sensitized mice was similar in the different animal groups (data not shown). Compared with +/+ mice, the number of I-A^b–brightFITC$^+$ cells in the draining lymph nodes was decreased in CCR2$^{-/-}$ but not in CCR5$^{-/-}$ mice (Fig. 4 A). The majority of the I-A^b–bright cells were DEC-205$^+$ (Fig. 4 B) and not B lymphocytes (by B220 staining; data not shown), indicating that most of the cells that stained brightly for I-A^b were DCs. Additionally, compared with +/+ mice, the number of FITC$^+$I-A^b–brightDEC-205$^+$ cells was lower in CCR2-null mice, but there was no difference in the numbers of FITC$^-$I-A^b–brightDEC-205$^+$ cells between +/+ and CCR2-null mice (Fig. 4 C). The proportion (mean percentage positive ± SD) of LCs that migrated to the draining lymph nodes in MIP-1α$^{-/-}$ mice (0.65 ± 0.14) was similar to that in +/+ mice (0.53 ± 0.17).

Collectively, our findings indicate that mice lacking CCR2 have a defect in LC migration. Contributing to this defect, the migrating LCs may be disproportionately retained in the subcapsular region, so that dispersion throughout the lymph node is delayed. Because CCR2-deficient mice have impaired macrophage recruitment (25–28), a theoretical argument could be made that the reduced migration of FITC-labeled LCs to the draining lymph nodes is merely a reflection of impaired macrophage/
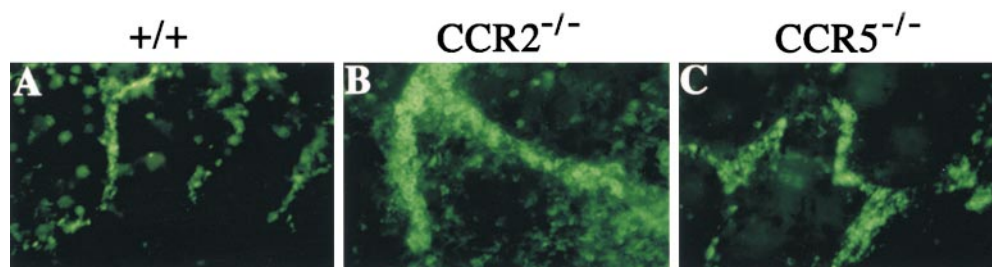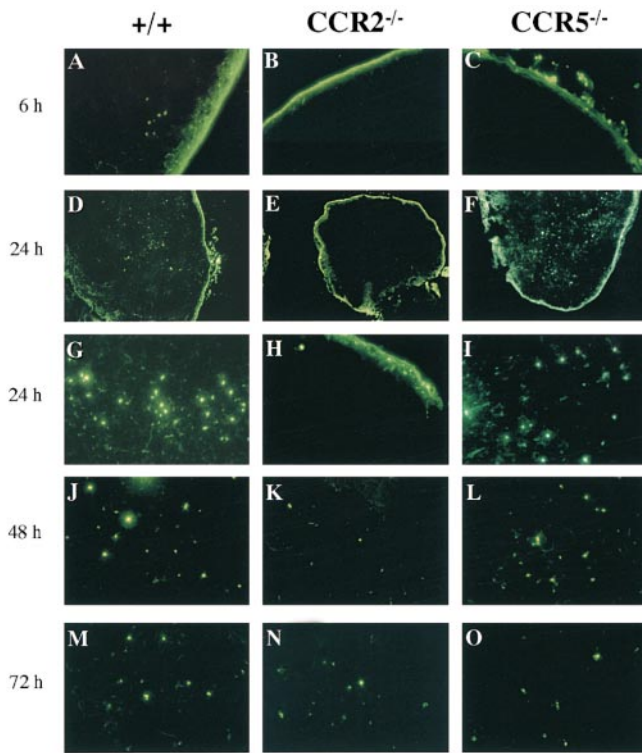

+/+   CCR2$^{-/-}$ CCR5$^{-/-}$

Figure 2. Disproportionately higher numbers of I-A^{b+} cells are found in the dermal layers from 72-h skin explants of CCR2-null mice. Dermal cords in ear explants of (A) +/+, (B) CCR2$^{-/-}$, and (C) CCR5$^{-/-}$ mice. LCs (I-A^{b+} cells) present in the dermal layer of 72-h ear explants were examined by immunofluorescence (A–C; original magnification: ×200).

| | +/+ | CCR2⁻/⁻ | CCR5⁻/⁻ |

Figure 3. Reduced migration of LCs to draining lymph nodes in CCR2-deficient mice after contact sensitization with FITC. (A–O) Time course of migration of FITC$^+$ LCs into lymph nodes. (A–C) 6, (D–I) 24, (J–L) 48, and (M–O) 72 h after painting of abdomen of +/+, CCR2$^{-/-}$, and CCR5$^{-/-}$ mice with FITC, the draining lymph nodes were collected and examined by fluorescence microscopy. Representative lymph node sections at these time points are shown. The original magnification shown is ×400 except in D–F, where it is ×100. A–C, D, F, and H are representative photomicrographs from the edge of the lymph node, whereas E depicts an entire lymph node. G, I, and J–O are from the center of the lymph nodes. The number of lymph node sections that contain FITC$^+$ LCs per total number of draining lymph node sections examined is shown below A–O (n = 3 mice per group per time point). A section with even a single FITC$^+$ cell was considered positive. Thus, for example, by this stringent criteria, in the CCR2$^{-/-}$ mice at 6 h, no lymph node sections contained any FITC$^+$ LCs, whereas 4 of 18 sections contained FITC$^+$ LCs at 24 h. A–C show localization of FITC$^+$ LCs to the periphery of the lymph nodes in A and C, but not in B. In E and H, a few FITC$^+$ LCs could be detected only in the periphery of the lymph node sections, whereas in D, F, G, I, and J–O, FITC$^+$ LCs were found dispersed throughout the lymph node sections. Note, the edges of the lymph nodes contain free FITC.

FITC+ lymph node sections

Time	+/+	CCR2⁻/⁻	CCR5⁻/⁻
6 h	7/23	0/29	2/30
24 h	15/23	4/18	18/24
48 h	22/22	8/17	8/10
72 h	10/26	5/12	6/21

monocyte recruitment. Furthermore, a case could be made that an additional confounding factor is the observation that monocytes may differentiate into DCs during migration into the lymphatic vessels (49). However, these confounding factors are unlikely to account for our findings of decreased LC migration in CCR2-null mice, as previous studies have clearly demonstrated that after FITC sensitiza-
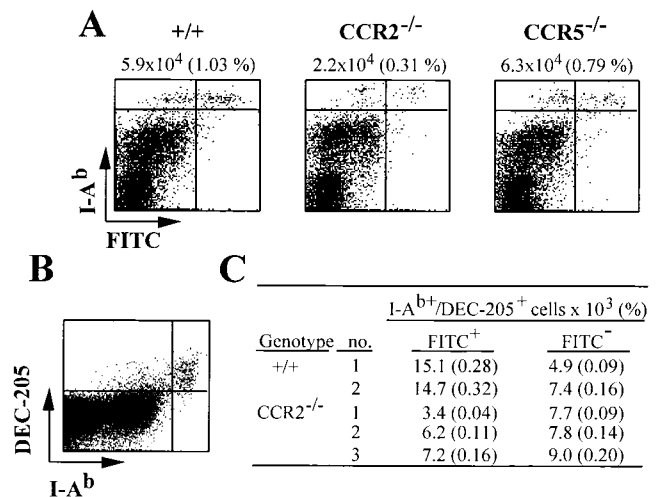

Figure 4. Impaired migration of LCs to the draining lymph nodes in CCR2$^{-/-}$ mice. (A) The ears of +/+, CCR2$^{-/-}$, and CCR5$^{-/-}$ mice were painted with FITC, and 24 h later, cells from two cervical lymph nodes were pooled and stained with PE-labeled anti–I-A^b mAb. Three animals per group were analyzed. Representative FACS$^®$ profile showing a reduction in the absolute number (and proportion) of FITC$^+$I-A^b– bright cells that migrated from the ear in CCR2$^{-/-}$ mice. The data are from one of three representative experiments. (B) Representative FACS$^®$ profile showing that most of the I-A^b–bright cells found in the upper-right quadrants in A also stain positive for DEC-205, suggesting that they represent LCs. The FACS$^®$ profile is from +/+ mice. (C) Reduced migration of DEC-205$^+$I-A^b$^+$FITC$^+$ cells in CCR2-null mice. Data were obtained by three-color cytometry analysis and are from two +/+ and three CCR2-null mice.

tion, the FITC$^+$ cells in the lymph node cells are derived entirely from the LC population (49, 50).

Reduced Th1-inducing DCs and Impaired Infection-induced Relocalization of CD11c$^+$ Cells in the Spleens of CCR2-deficient Mice. Characterization of splenic DC subpopulations by phenotypic, functional, and histological parameters has identified two major DC subsets in the spleen and has shown that these DC subsets reside in distinct microenvironments (20, 22). By immunohistochemistry, CCR2$^{-/-}$ mice had reduced numbers of CD11c$^+$ cells compared with +/+ and CCR5-null mice (data not shown). These findings were confirmed by three-color flow cytometry (Table I), and the maximum decrease was in the subpopulation of DCs whose staining pattern was CD11c$^+$ CD8α$^+$CD11b$^-$ (Table I). Although the mean number of CD11c$^+$CD8α$^-$CD11b$^+$–staining DCs also appeared lower in CCR2-null mice, these differences were not statistically significant.

There is evidence that after activation of splenic DCs in vivo, such as after administration of LPS, there is conversion of immature to mature DCs and relocalization of marginal zone DCs into the T cell areas (51). Activation of DCs after an infection is a more physiological model for examining this activation-induced relocalization of DCs, and would also place the interpretation of the immune responses observed in CCR2-null mice after infection with *L. major* in a more appropriate context. By three-color flow

Table I. *CD11c$^+$ DC Subsets in +/+, CCR2$^{-/-}$, and CCR5$^{-/-}$ Mice*

	Genotype	CD11c$^+$CD8α^+CD11b$^-$		CD11c$^+$CD8α^-CD11b$^+$	
		Percentage positive	Number	Percentage positive	Number
			($\times 10^6$)		*($\times 10^6$)*
Uninfected	+/+	1.04 ± 0.19	1.48 ± 0.53	2.44 ± 0.89	3.53 ± 1.86
	CCR2$^{-/-}$	0.49 ± 0.10*	0.72 ± 0.20	1.58 ± 0.17	2.31 ± 0.19
	CCR5$^{-/-}$	0.92 ± 0.13	1.52 ± 0.17	2.77 ± 0.33	4.60 ± 0.54
Infected	+/+	1.22 ± 0.04	1.22 ± 0.12	1.31 ± 0.22	1.30 ± 0.08
	CCR2$^{-/-}$	0.79 ± 0.16‡	0.51 ± 0.10*	0.67 ± 0.23‡	0.43 ± 0.14*

Three-color flow cytometry analysis was used to determine the proportion and absolute numbers (mean ± SD) of CD11c$^+$CD8α^-CD11b$^+$ DCs in spleen cell suspensions.
*$P < 0.05$, difference from +/+ mice.
‡$P < 0.01$, difference from +/+ mice.

cytometry, 7-d–infected CCR2-null mice had lower numbers of CD11c$^+$CD8α^+CD11b$^-$ and CD11c$^-$CD8α^-CD11b$^+$ DC subsets compared with infected +/+ mice (Table I). Analagous to the findings in LPS-treated mice (51), by immunohistochemistry we found that infected +/+ mice had increased numbers of CD11c$^+$ cells in the T cell areas compared with uninfected +/+ mice (data not shown). However, compared with infected +/+ mice, there was a paucity of CD11c$^+$ cells in the periarteriolar sheaths of the infected CCR2-null mice. Taken together, our data suggest that CCR2 is an important determinant for the localization of CD8α^+ splenic DCs and the activation-induced movement of DCs into the T cell areas of the spleen.

Normal Ag-presenting Capacity of LCs/DCs in CCR2$^{-/-}$ and CCR5$^{-/-}$ Mice. To determine whether LCs in CCR2$^{-/-}$ mice were functionally active, DCs were purified from draining lymph nodes of FITC-sensitized mice and examined for their capacity to activate allogeneic T cells. Allogeneic BALB/c T cells were isolated and mixed with +/+, CCR2$^{-/-}$, or CCR5$^{-/-}$ DCs (data not shown). DCs isolated from CCR2$^{-/-}$ and CCR5$^{-/-}$ mice were similar to those from +/+ mice in their ability to

stimulate allogeneic T cells. To analyze further the Ag-presenting capacity of DCs from knockout mice, KLH-pulsed spleen DCs from +/+, CCR2$^{-/-}$, or CCR5$^{-/-}$ mice were incubated with purified CD3$^+$ T cells derived from +/+ mice immunized with KLH. KLH-pulsed spleen DCs isolated from +/+, CCR2$^{-/-}$, or CCR5$^{-/-}$ mice were equally effective in stimulating Ag-specific proliferation of CD3$^+$ T cells (data not shown). Similar results were also obtained by using KLH-pulsed bone marrow–derived DCs in Ag-specific syngeneic proliferation assays (data not shown).

CCR2-deficient Mice Are Susceptible to L. major Infection and Develop a Predominant Th2-like Response. The contribution of the aforementioned defects in DC migration and localization in CCR2-null mice to the development of a protective cell-mediated immune response to *L. major* infection was next examined. The genetic background of the wild-type and knockout mice used in these studies is composed of two resistant strains, C57BL/6 and 129/J (52). Control animals and mice deficient in CCR5 or MIP-1α retained the *L. major*–resistant phenotype as demonstrated by mild, self-resolving ear swelling (Fig. 5 A). In contrast, CCR2-null mice failed to control *L. major*, and the ear
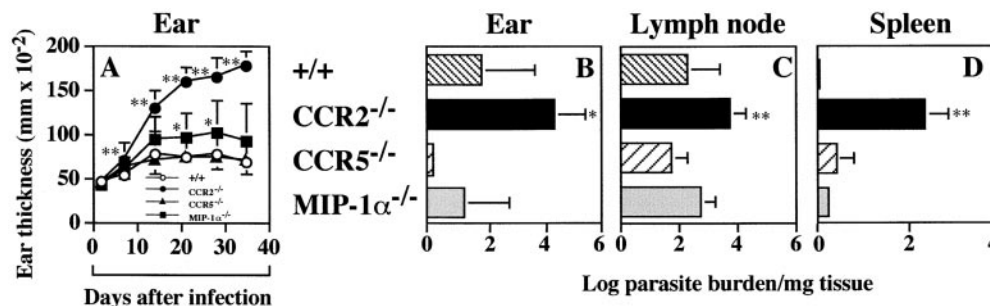

Figure 5. CCR2$^{-/-}$ mice showed marked sensitivity to *L. major* infection. (A) Thickness of the ears of wild-type (+/+; ○), CCR2$^{-/-}$ (●), CCR5$^{-/-}$ (▲), or MIP-1$\alpha^{-/-}$ (■) mice after intradermal inoculation of *L. major*. Results are the mean ± SD for 10 mice (2 d and 1 wk) or 5 mice (2, 3, 4, and 5 wk). (B–D) Parasite burden in the ears, draining lymph nodes, and spleens. Results are the mean ± SD for five mice, and are from one of two representative experiments. *$P < 0.05$ and **$P < 0.01$, difference from +/+ mice.

thickness continued to increase during the course of infection (Fig. 5 A). 1 and 3 wk after infection, there was no significant difference in the parasite burden between the knockout and +/+ mice (data not shown). However, at 5 wk after infection, the highest parasite burden in the ears, draining lymph nodes, and spleens was in mice deficient in CCR2 (Fig. 5, B–D). Parasites could be detected in 90% of the infected spleens of CCR2$^{-/-}$ mice. In contrast, none of the +/+ mice and only 30% of CCR5$^{-/-}$ or MIP-1$\alpha^{-/-}$ mice had parasites in the spleen. Thus, progression to disease beyond the draining lymph nodes (i.e., visceralization to other organs) was greatest in mice lacking CCR2.

To assess the Th effector cell phenotype in the infected animals, in vitro Ag-specific cytokine production was measured 1 and 5 wk after infection (Fig. 6, A–H). Previous studies have shown that the early development of Th2 (IL-4) but lower Th1 (IFN-γ) responses underlie susceptibility to infection (29). Concordant with these observations, 1 wk after infection, the Ag-specific production of IFN-γ in the draining lymph nodes and spleens of CCR2-null mice

Figure 6. Ag-specific production of IL-4 and IFN-γ by lymph node and spleen cells after 1 wk (A–D) or 5 wk (E–H) of *L. major* infection in wild-type (+/+; ○), CCR2$^{-/-}$ (●), CCR5$^{-/-}$ (▲), or MIP-1$\alpha^{-/-}$ (■) mice. Horizontal lines in each panel indicate the mean cytokine production level in wild-type mice. Each symbol represents the Ag-specific cytokine levels produced from a single mouse. One of three representative experiments is shown. I shows *L. major*–specific total Igs, IgG1, and IgG2a levels in serum of +/+, CCR2$^{-/-}$, CCR5$^{-/-}$, and MIP-1$\alpha^{-/-}$ mice after 5 wk of infection. Data represent OD obtained after a 400-fold dilution of the serum, and the data are expressed as mean ± SD. (n = five mice per group). One of two representative experiments is shown. †$P <$ 0.05 and ††$P <$ 0.01, difference from +/+ mice.

was lower compared with +/+ mice (Fig. 6, C and D). Conversely, Ag-specific IL-4 production was higher in the draining lymph nodes of CCR2-null mice (Fig. 6 A). At later stages of infection, CCR2-null mice produced high levels of both IL-4 and IFN-γ (Fig. 6, E–H). Previous studies have demonstrated that although a Th1 response is sufficient to protect against cutaneous leishmaniasis, the induction of a simultaneous Th2 response abrogates the Th1 effector function (29, 53).

In contrast to CCR2-null mice, a Th2-biased cytokine profile was not evident in mice deficient in either CCR5 or MIP-1α. CCR5-null mice had higher levels of IFN-γ in the spleen and lymph nodes 1 and 5 wk after infection (Fig. 6, G and H). At 5 wk after infection, CCR5-null mice produced significantly lower levels of Ag-specific IL-4 in the spleen (Fig. 6 F).

Additional evidence for a dominant Th2 phenotype in CCR2-null mice came from the finding that 5 wk after infection, the Ag-specific Ig and IgG1 levels were significantly higher in the CCR2$^{-/-}$ mice compared with +/+, CCR5$^{-/-}$, or MIP-1$\alpha^{-/-}$ mice (Fig. 6 I). The levels of IgG2a, an Ig typically associated with Th1-biased responses, were similar in the different animal groups (Fig. 6 I). Ag-specific IgG3 and IgE were not detectable (data not shown). However, total IgE levels were ~11-fold higher in CCR2-deficient mice compared with wild-type mice (data not shown).

Marked Neutrophilic Inflammation in CCR2$^{-/-}$ Mice Infected with L. major. Persistent neutrophilic inflammation in the infected ears is one of the hallmarks of the pathological changes that occur in mice susceptible to experimental cutaneous leishmaniasis (32). Concordant with these observations, we found that the ears of 6-wk–infected CCR2$^{-/-}$ mice were remarkable for a prominent neutrophilic infiltrate with areas of necrosis, whereas the ears of infected +/+, CCR5$^{-/-}$, or MIP-1$\alpha^{-/-}$ mice had scattered infiltrating monocytes and fibroblasts (Fig. 7, A and B). Notably, by histology, neutrophils comprised ~80% of the total inflammatory infiltrate in CCR2$^{-/-}$ mice. We took advantage of the ear skin explant model and flow cytometry to quantify the magnitude and kinetics of neutrophil recruitment in CCR2-null mice. At both 1 and 7 d after infection, neutrophils comprised >70% of the total number of cells in the infected ears of CCR2-null mice (Fig. 7 B). In contrast, in wild-type and CCR5-null mice, neutrophils comprised ~40–60% of all cells in the infected ears 1 d after infection, and <20% at day 7 after infection (Fig. 7 B). Taken together, these findings suggest that the inflammatory response in CCR2-null mice on a genetically resistant background is remarkably reminiscent of the acute inflammatory response seen during *L. major* infection in susceptible BALB/c mice (32).

Enhanced B Cell Outgrowth and Increased BLC mRNA Expression in CCR2-deficient Mice. Previous studies have indicated that an outgrowth of B cells during the acute phase of *L. major* infection correlates with a Th2-type dominance (30). 1 wk after infection with *L. major*, compared with +/+ mice, in sections stained for B220$^+$ cells the B cell follicles
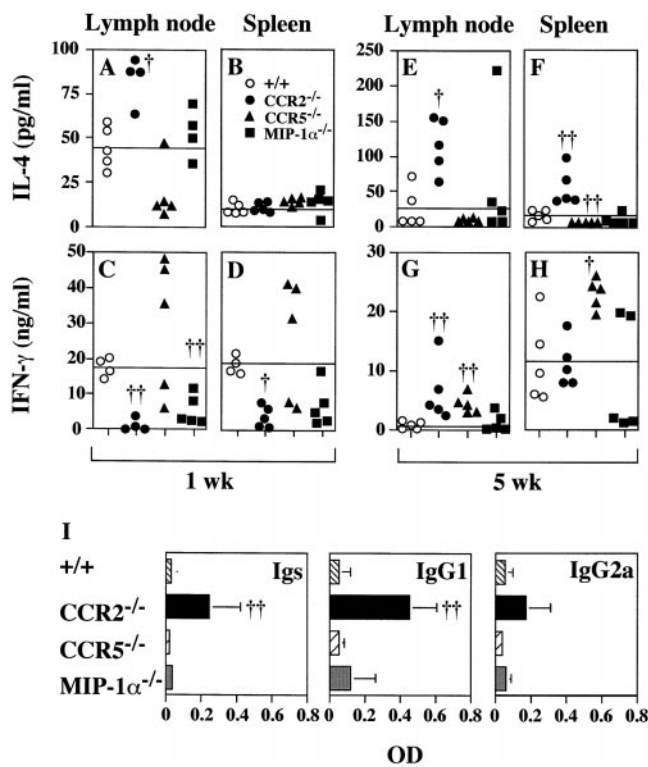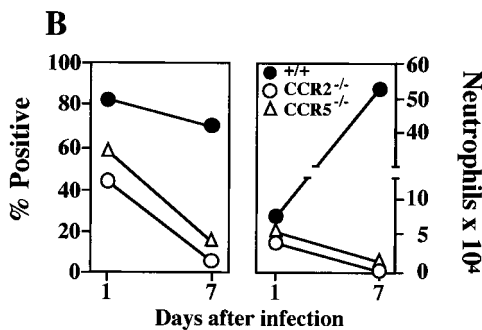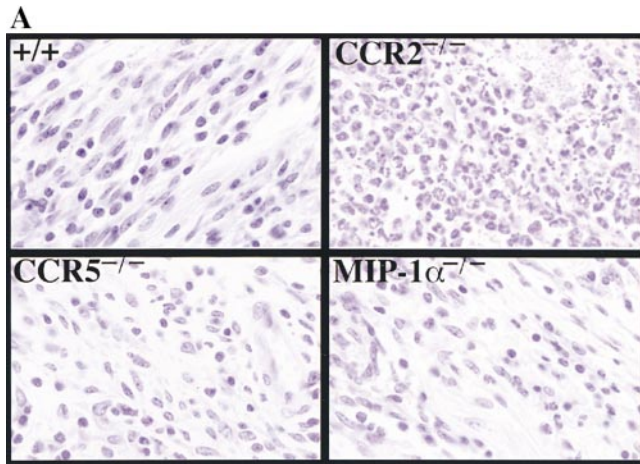
Figure 7. Marked neutrophilic inflammation in mice deficient in CCR2. (A) The histopathological sections (hematoxylin and eosin; original magnification: ×400) are from mice infected for 5 wk with *L. major.* Abundant organisms admixed with areas of necrosis, karryohectic cellular fragments, and polymorphonuclear leukocytes including eosinophils were found in CCR2$^{-/-}$ mice. In contrast, the ears from +/+, CCR5$^{-/-}$, and MIP-1α$^{-/-}$ mice had fibroblasts with scattered cellular infiltrates that consisted of mononuclear cells, epitheloid histiocytes, lymphocytes, and plasmacytoid cells. Necrosis was absent in these three groups of mice. (B) Marked recruitment of neutrophils to the ears of CCR2-null mice after intradermal infection with *L. major.* 1 and 7 d after *L. major* infection, the cells that emigrated from ear skin explants were stained with FITC-labeled anti-I-A^b mAb and PE-labeled anti–Ly-6G mAb. Percentage (left) and total number (right) of neutrophils (Ly-6G brightI-A^{b-}) among all cells that emigrated from skin explants of +/+ (○), CCR2$^{-/-}$ (●), and CCR5$^{-/-}$ (△) mice are shown. Results from one of three representative experiments are shown.

Figure 8. Enhanced B cell outgrowth and increased BLC mRNA expression in the lymph nodes of *L. major*–infected CCR2-deficient mice. (A and B) Lymph nodes from 7 d–infected +/+ and CCR2$^{-/-}$ mice were stained with anti-B220 mAb (brown) and TUNEL (blue) (original magnification: ×100). (C and D) Increased BLC mRNA expression in CCR2-null mice. BLC mRNA expression was determined in uninfected cervical lymph nodes or in the draining cervical lymph nodes after 1 d of *L. major* infection in wild-type and CCR2-null mice. (C) 20 μg of total RNA was purified, and Northern blots were hybridized with a radiolabeled BLC-specific probe. The autoradiographs were obtained after 4 d (BLC) or 1 d (GAPDH) of exposure. (D) Relative BLC mRNA levels were determined from the mRNA blots of the infected animals shown in A. Data from individual mice are shown (○, +/+ mice) and (●, CCR2$^{-/-}$ mice), and the bar represents the mean. Data from one of two representative experiments are shown.

in the draining lymph nodes in CCR2$^{-/-}$ mice were very enlarged (data not shown). Double labeling for B220 and apoptotic cells (TUNEL technique; Fig 8, A and B) showed a marked increase in TUNEL$^+$ cells in the B cell areas, suggestive of increased B cell proliferation.

Because the B cell outgrowth was so prominent in CCR2-null mice, we tested the possibility that this may be due to higher expression of BLC, a B cell–specific chemokine (15, 17). Stromal cells, including follicular DCs found in the B cell regions of all secondary lymphoid tissue, produce BLC (15, 54), and several factors have been shown to influence the expression of BLC (15, 17, 55). CCR2-deficient mice appeared to be primed for enhanced B cell outgrowth after infection, as compared with +/+ mice,
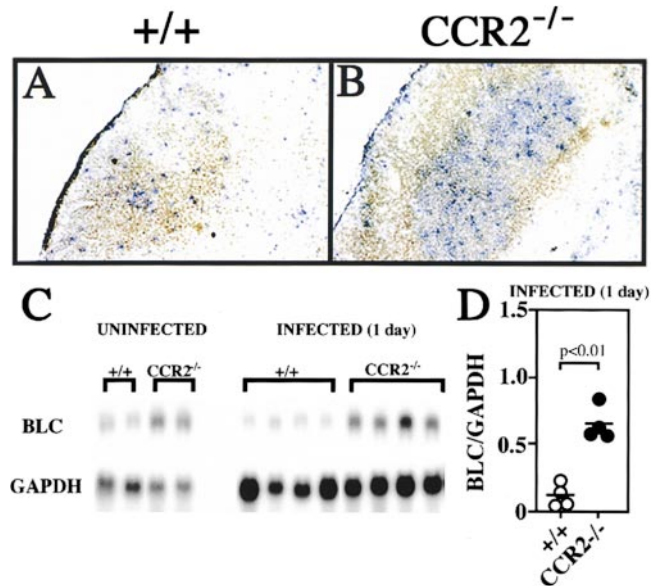
the lymph nodes derived from 1-d *L. major*–infected CCR2-deficient mice expressed significantly higher amounts of BLC mRNA (Fig. 8, C and D). Interestingly, lymph nodes of uninfected CCR2-null mice also expressed higher levels of BLC mRNA (Fig. 8 C). Studies are underway to determine whether signaling via CCR2 negatively regulates BLC expression directly or indirectly (i.e., by inhibiting the maturation of BLC-expressing stromal cells, such as follicular DCs).

Discussion

The trafficking events that bring together T cells, B lymphocytes, and DCs—the major participants of cellular and humoral immune responses—form a tightly orchestrated and complex process for which a key role for the chemokine system has emerged (3–8). In this study, we demonstrate that CCR2 is an important determinant of DC/LC migration and localization, especially in the localization of CD8α Th1-inducing splenic DCs, and is required to generate protective cell-mediated immune responses to *L. major* infection. In contrast, major defects in DC migration or localization or in host responses to *L. major* infection were not observed in mice that have an identical genetic back-

ground but are deficient in CCR5 or MIP-1α. The concurrent analysis of three knockout mice on identical *L. major*–resistant genetic backgrounds also affords some insights into the issue of redundancy versus specificity of distinct chemokine receptor–ligand pairs. Despite sharing overlapping ligand/agonist profiles (7, 56), the in vivo function of CCR2 cannot be replaced by CCR5, whereas it would appear that the converse is not true, indicating that in the genetic background tested, CCR2 has nonredundant properties with regard to Th1/Th2 balance in experimental cutaneous leishmaniasis.

Where do CCR2 and CCR5 fit into the proposed complex model of LC/DC navigation (3, 4, 8)? Because contact sensitization induced by FITC skin painting is known to induce DC maturation and mobilization (49, 50), and because CCR2 and CCR5 are thought to be involved primarily in the trafficking of immature DCs, the finding of marked impairment of LC migration in CCR2-deficient mice was unanticipated. How then does one reconcile these findings in the context of the proposed model of LC/DC migration? There are several lines of evidence to suggest that CCR2 expression influences the migration of both immature and mature LCs. First, in addition to being an inducible or "inflammatory" chemokine, monocyte chemoattractant protein (MCP)-1 is constitutively expressed by many tissues (57). Indeed, at least in human DCs, MCP-1 is expressed by immature DCs, and its expression is strongly upregulated in mature DCs (10). Thus, because CCR2 is the only known high-affinity receptor for MCP-1, the CCR2–MCP-1 axis may influence both phases of LC migration. Second, although a switch in chemokine receptor profile during DC maturation is clearly an important determinant in DC migration, studies with in vitro–derived human or murine DCs indicate that this switch may not be an all-or-none phenomenon. In in vitro expression studies, murine CCR2 is constitutively expressed on control/immature DCs, and although after exposure to TNF-α the levels of CCR2 mRNA decline significantly, CCR2 expression on activated DCs remains detectable (9). On the other hand, in these experiments, murine CCR5 expression on activated DCs was not detectable (9). Thus, the continued expression of murine CCR2 but not CCR5 on mature/activated DCs could influence the migration of maturing murine DCs and is consistent with our in vivo findings of reduced migration of activated LCs to the draining lymph nodes. Additionally, the changes in receptor profiles observed in in vitro–derived DCs (CD34+ stem cell– or bone marrow–derived DCs) may not accurately mirror the changes that occur on native DCs in vivo. Also, the efficiency with which this switch in receptor expression occurs in response to activation may be highly dependent on the stimulus (9, 10), and thus the results found after in vitro and in vivo DC activation are unlikely to be the same.

Defects in DC biology in CCR2-deficient mice were not restricted to a decrease in LC migration. In contrast to the fairly global defect in DC localization in the spleen and lymph nodes of mice lacking expression of the second-ary lymphoid tissue chemokine (16), DC localization in CCR2-deficient mice appeared to be relatively specific to the CD8α+ lineage of DCs in the spleen. The finding of reduced numbers of CD8α+ DCs is especially intriguing because recent studies suggest that the nature of the DC that presents Ags to naive T cells may dictate the class selection (Th1/Th2) of the adaptive immune response (20–22). CD8α+ DCs have been shown to drive the development of Th1-type immune responses required to control intracellular infections, whereas CD8α− DCs induce the differentiation of Th2-type responses that are important in the control of extracellular infections (21). Additionally, restriction of the DC defects to LC migration and localization of CD8α+ DCs is interesting in the context of recent studies suggesting that LCs also belong to the CD8α+ DC lineage (58).

Our studies in knockout mice on an *L. major*–resistant genetic background provide insights into the role of CCR2, CCR5, and MIP-1α in cure versus susceptibility to experimental cutaneous leishmaniasis. Studies of infection with *L. major* have established a paradigm for the role of different T helper subsets during infection (29). Early production of IFN-γ and IL-12 is responsible for Th1 development and disease resistance, whereas an early IL-4 response induces Th2 cell development in susceptible mice. Susceptible BALB/c mice permit a rapid dissemination of *L. major* parasites to visceral organs within the first 10–24 h of infection, whereas in resistant strains such as C57BL/6, the parasites are restricted to the site of infection and the draining lymph node. There were striking similarities in the disease expression of *L. major* infection in BALB/c mice and CCR2-deficient mice. This included progressive and disseminated infection, presence of high IL-4 levels during the early and later phases of the immune responses, higher production of IgG1, prominent local neutrophilic inflammation, and enhanced B cell outgrowth that may be related to increased BLC expression. In contrast, mice deficient in CCR5 or MIP-1α had phenotypes similar to those of the *L. major*–resistant genetic background mice.

In a recent report, Gu et al. (59) reported that mice lacking MCP-1 have impaired Th2 responses and resist *L. major* infection. These findings are the opposite of those that we observed in *L. major*–infected CCR2-deficient mice. Several explanations can be invoked to explain these contrasting and paradoxical findings, including the possibility that MCP-3 and MCP-5, two additional high-affinity ligands for CCR2, might induce Th1 polarization in MCP-1–deficient mice. Also, differences in the *L. major* disease phenotype in other ligand–receptor pairs have been noted (60). However, before making firm conclusions about the contrasting functions of MCP-1 and CCR2, several important caveats should be considered. First, some of the comparisons between MCP-1 and CCR2 knockout mice are in contrasting genetic backgrounds. For example, the *L. major* infection studies reported by Gu et al. (59) were in the susceptible background (BALB/c), whereas our studies were in the resistant background (C57BL/6 × 129). Several studies have documented that the same mutation can have

markedly different phenotypes when placed on different genetic backgrounds (61, 62). This variation is due to different alleles at modifying loci in various inbred strains. Second, extensive studies in mice deficient for IL-4 or its receptor (IL-4Rα) have shown that the disease outcomes to *L. major* infection are heavily dependent on the parasite substrain (63, and references therein). Thus, to resolve the contrasting *L. major* phenotype in MCP-1– and CCR2-deficient mice, it will be necessary to conduct concurrent studies of these two knockouts on similar genetic backgrounds using identical *L. major* strains.

Can a direct connection be made between the Th2-biased *L. major*–susceptible phenotype in CCR2-null mice and the DC defects? Given the broad array of complex DC defects, providing experimental evidence that any one of these DC defects is directly responsible for the susceptible phenotype is a challenging task. It is more likely that in CCR2-null mice, the sum of these DC defects in conjunction with enhanced susceptibility to B cell expansion collectively contribute to this phenotype. Nevertheless, based on our current findings, two possible scenarios can be envisaged by which the observed defects can affect an *L. major* Ag–specific T cell–dependent response, and consequently susceptibility to infection.

The first scenario ties in the potential immunological consequences of the observed defects at the level of lymph node, i.e., impaired Ag presentation due to inadequate migration of Ag-bearing LCs and enhanced B cell outgrowth. For mature DCs to function in an immunogenic manner, it is clear that they need to interact rapidly with Ag-specific T cells. In an elegant study, Inguilli et al. (64) demonstrated that there is a limited window of time during which Ag-loaded DCs interact with T cells. Ag (OVA)-bearing DCs were found to interact with naive Ag-specific T cells within the T cell–rich regions of lymph nodes during the first 24 h after injection of ex vivo Ag-pulsed DCs, and that 48 h after injection, Ag-pulsed DCs disappeared from the lymph nodes (64). It was during this critical 0–24-h period that LCs from CCR2-null mice had the greatest impairment in migration, and it is known that the factors that influence Th cell differentiation after *L. major* infection are operative within the first hours or days of infection (65, 66). Studies in other experimental systems have also shown that the early events in the differentiation of naive CD4$^+$ T cells determine the nature of cytokines produced, and thus influence Th1/Th2 balance (67). Concurrent with this defect, we observed that CCR2-null mice are primed for increased B cell outgrowth. This observation is important in the context that, in general, macrophages and DCs preferentially induce IFN-γ and IL-2 secretion, whereas B cells are more efficient in activating IL-4 production (68). Additionally, Palanivel et al. (30) demonstrated that B cell outgrowth and Ag-specific production of Th2 cytokines correlate with Th2 dominance. Thus, in the context of these observations, it is not inconceivable that the combination of impaired Ag presentation due to reduced migration of *Leishmania* Ag-loaded DCs to the draining lymph nodes and the propensity for increased B

cell expansion could lead to a skewed Th2 phenotype in CCR2-null mice.

In the second scenario, the altered splenic microenvironment in naive, uninfected CCR2-null mice (i.e., reduced Th1-inducing DCs in the T cell areas) and impaired infection-induced relocalization of DCs from the marginal zone to the T cell areas also provide another connection to the Th2-biased *L. major*–susceptible phenotype. Interestingly, 1 wk after infection, the Ag-specific production of IFN-γ was lower in the spleens of CCR2-null mice, and this inability to generate a Th1 response may be attributable, in part, to reduced numbers of Th1-inducing splenic DCs. The possibility of these alterations in skewing the Th balance is also highlighted by the observation that Th1 and Th2 cells home to distinct microenvironments of the spleen, and that this unique cellular migration pattern may be due to the differential expression patterns of chemokine receptors (69).

In summary, the findings presented herein demonstrate that CCR2 plays a key role in the migration of DCs/LCs in vivo, as well as DC/LC localization. The preferential decrease in CD8α, Th1-inducing splenic DCs, and the infection-induced block in DC relocalization would suggest that CCR2, in addition to CCR7, is important in maintaining functional microenvironments in secondary lymphoid organs. Regardless of whether these DC defects contribute directly or indirectly to the striking Th2-biased phenotype, our studies demonstrate a central role for CCR2 in regulating Th1/Th2 balance in experimental cutaneous leishmaniasis in mice that are normally resistant to this infection.

References

1. Banchereau, J., and R.M. Steinman. 1998. Dendritic cells and the control of immunity. *Nature.* 392:245–252.
2. Butcher, E.C., M. Williams, K. Youngman, L. Rott, and M. Briskin. 1999. Lymphocyte trafficking and regional immunity. *Adv. Immunol.* 72:209–253.
3. Cyster, J.G. 1999. Chemokines and cell migration in secondary lymphoid organs. *Science.* 286:2098–2102.
4. Cyster, J.G. 1999. Chemokines and the homing of dendritic

cells to the T cell areas of lymphoid organs. *J. Exp. Med.* 189: 447–450.

5. Sallusto, F., B. Palermo, D. Lenig, M. Miettinen, S. Matikainen, I. Julkunen, R. Forster, R. Burgstahler, M. Lipp, and A. Lanzavecchia. 1999. Distinct patterns and kinetics of chemokine production regulate dendritic cell function. *Eur. J. Immunol.* 29:1617–1625.

6. Sallusto, F., and A. Lanzavecchia. 1999. Mobilizing dendritic cells for tolerance, priming, and chronic inflammation. *J. Exp. Med.* 189:611–614.

7. Kim, C.H., and H.E. Broxmeyer. 1999. Chemokines: signal lamps for trafficking of T and B cells for development and effector function. *J. Leukoc. Biol.* 65:6–15.

8. Melchers, F., A.G. Rolink, and C. Schaniel. 1999. The role of chemokines in regulating cell migration during humoral immune responses. *Cell.* 99:351–354.

9. Vecchi, A., L. Massimiliano, S. Ramponi, W. Luini, S. Bernasconi, R. Bonecchi, P. Allavena, M. Parmentier, A. Mantovani, and S. Sozzani. 1999. Differential responsiveness to constitutive vs. inducible chemokines of immature and mature mouse dendritic cells. *J. Leukoc. Biol.* 66:489–494.

10. Sallusto, F., P. Schaerli, P. Loetscher, C. Schaniel, D. Lenig, C.R. Mackay, S. Qin, and A. Lanzavecchia. 1998. Rapid and coordinated switch in chemokine receptor expression during dendritic cell maturation. *Eur. J. Immunol.* 28:2760–2769.

11. Tang, H.L., and J.G. Cyster. 1999. Chemokine up-regulation and activated T cell attraction by maturing dendritic cells. *Science.* 284:819–822.

12. Forster, R., A.E. Mattis, E. Kremmer, E. Wolf, G. Brem, and M. Lipp. 1996. A putative chemokine receptor, BLR1, directs B cell migration to defined lymphoid organs and specific anatomic compartments of the spleen. *Cell.* 87:1037–1047.

13. Forster, R., A. Schubel, D. Breitfeld, E. Kremmer, I. Renner-Muller, E. Wolf, and M. Lipp. 1999. CCR7 coordinates the primary immune response by establishing functional microenvironments in secondary lymphoid organs. *Cell.* 99:23–33.

14. Cyster, J.G. 2000. Leukocyte migration: scent of the T zone. *Curr. Biol.* 10:R30–R33.

15. Cyster, J.G., V.N. Ngo, E.H. Ekland, M.D. Gunn, J.D. Sedgwick, and K.M. Ansel. 1999. Chemokines and B-cell homing to follicles. *Curr. Top. Microbiol. Immunol.* 246:87–92.

16. Gunn, M.D., S. Kyuwa, C. Tam, T. Kakiuchi, A. Matsuzawa, L.T. Williams, and H. Nakano. 1999. Mice lacking expression of secondary lymphoid organ chemokine have defects in lymphocyte homing and dendritic cell localization. *J. Exp. Med.* 189:451–460.

17. Gunn, M.D., V.N. Ngo, K.M. Ansel, E.H. Ekland, J.G. Cyster, and L.T. Williams. 1998. A B-cell-homing chemokine made in lymphoid follicles activates Burkitt's lymphoma receptor-1. *Nature.* 391:799–803.

18. Legler, D.F., M. Loetscher, R.S. Roos, I. Clark-Lewis, M. Baggiolini, and B. Moser. 1998. B cell-attracting chemokine 1, a human CXC chemokine expressed in lymphoid tissues, selectively attracts B lymphocytes via BLR1/CXCR5. *J. Exp. Med.* 187:655–660.

19. Berger, E.A., P.M. Murphy, and J.M. Farber. 1999. Chemokine receptors as HIV-1 coreceptors: roles in viral entry, tropism, and disease. *Annu. Rev. Immunol.* 17:657–700.

20. Shortman, K., and C. Caux. 1997. Dendritic cell development: multiple pathways to nature's adjuvants. *Stem Cells.* 15: 409–419.

21. Maldonado-Lopez, R., T. De Smedt, P. Michel, J. Godfroid, B. Pajak, C. Heirman, K. Thielemans, O. Leo, J. Urbain, and M. Moser. 1999. CD8α^+ and CD8α^- subclasses of dendritic cells direct the development of distinct T helper cells in vivo. *J. Exp. Med.* 189:587–592.

22. Pulendran, B., J. Lingappa, M.K. Kennedy, J. Smith, M. Teepe, A. Rudensky, C.R. Maliszewski, and E. Maraskovsky. 1997. Developmental pathways of dendritic cells in vivo: distinct function, phenotype, and localization of dendritic cell subsets in FLT3 ligand-treated mice. *J. Immunol.* 159:2222–2231.

23. Moll, H., S. Flohe, and M. Rollinghoff. 1995. Dendritic cells in *Leishmania major*-immune mice harbor persistent parasites and mediate an antigen-specific T cell immune response. *Eur. J. Immunol.* 25:693–699.

24. Moll, H., H. Fuchs, C. Blank, and M. Rollinghoff. 1993. Langerhans cells transport *Leishmania major* from the infected skin to the draining lymph node for presentation to antigen-specific T cells. *Eur. J. Immunol.* 23:1595–1601.

25. Boring, L., J. Gosling, S.W. Chensue, S.L. Kunkel, R.V. Farese, Jr., H.E. Broxmeyer, and I.F. Charo. 1997. Impaired monocyte migration and reduced type 1 (Th1) cytokine responses in C-C chemokine receptor 2 knockout mice. *J. Clin. Invest.* 100:2552–2561.

26. Kurihara, T., G. Warr, J. Loy, and R. Bravo. 1997. Defects in macrophage recruitment and host defense in mice lacking the CCR2 chemokine receptor. *J. Exp. Med.* 186:1757–1762.

27. Warmington, K.S., L. Boring, J.H. Ruth, J. Sonstein, C.M. Hogaboam, J.L. Curtis, S.L. Kunkel, I.R. Charo, and S.W. Chensue. 1999. Effect of C-C chemokine receptor 2 (CCR2) knockout on type-2 (schistosomal antigen-elicited) pulmonary granuloma formation: analysis of cellular recruitment and cytokine responses. *Am. J. Pathol.* 154:1407–1416.

28. Kuziel, W.A., S.J. Morgan, T.C. Dawson, S. Griffin, O. Smithies, K. Ley, and N. Maeda. 1997. Severe reduction in leukocyte adhesion and monocyte extravasation in mice deficient in CC chemokine receptor 2. *Proc. Natl. Acad. Sci. USA.* 94:12053–12058.

29. Jones, D.E., M.M. Elloso, and P. Scott. 1998. Host susceptibility factors to cutaneous leishmaniasis. *Front. Biosci.* 3:D1171–D1180.

30. Palanivel, V., C. Posey, A.M. Horauf, W. Solbach, W.F. Piessens, and D.A. Harn. 1996. B-cell outgrowth and ligand-specific production of IL-10 correlate with Th2 dominance in certain parasitic diseases. *Exp. Parasitol.* 84:168–177.

31. Sacks, D.L., P.A. Scott, R. Asofsky, and F.A. Sher. 1984. Cutaneous leishmaniasis in anti-IgM-treated mice: enhanced resistance due to functional depletion of a B cell-dependent T cell involved in the suppressor pathway. *J. Immunol.* 132: 2072–2077.

32. Beil, W.J., G. Meinardus-Hager, D.C. Neugebauer, and C. Sorg. 1992. Differences in the onset of the inflammatory response to cutaneous leishmaniasis in resistant and susceptible mice. *J. Leukoc. Biol.* 52:135–142.

33. Sato, N., W.A. Kuziel, P.C. Melby, R.L. Reddick, V. Kostecki, W. Zhao, N. Maeda, S.K. Ahuja, and S.S. Ahuja. 1999. Defects in the generation of IFN-gamma are overcome to control infection with *Leishmania donovani* in CC chemokine receptor (CCR) 5-, macrophage inflammatory protein-1 alpha-, or CCR2-deficient mice. *J. Immunol.* 163:5519–5525.

34. Cook, D.N., M.A. Beck, T.M. Coffman, S.L. Kirby, J.F. Sheridan, I.B. Pragnell, and O. Smithies. 1995. Requirement

of MIP-1 alpha for an inflammatory response to viral infection. *Science.* 269:1583–1585.

35. Melby, P.C., F.A. Neva, and D.L. Sacks. 1989. Profile of human T cell response to leishmanial antigens. Analysis by immunoblotting. *J. Clin. Invest.* 83:1868–1875.

36. Sacks, D.L., and P.C. Melby. 1998. Animal models for the analysis of immune responses to leishmaniasis. *In* Current Protocols in Immunology. J.E. Coligan, A.M. Kruisbeek, D.H. Marguiles, E.M. Shevach, and W. Strober, editors. John Wiley & Sons, Inc., New York. 19.2.1–19.2.20.

37. Ahuja, S.S., R.L. Reddick, N. Sato, E. Montalbo, V. Kostecki, W. Zhao, M.J. Dolan, P.C. Melby, and S.K. Ahuja. 1999. Dendritic cell (DC)-based anti-infective strategies: DCs engineered to secrete IL-12 are a potent vaccine in a murine model of an intracellular infection. *J. Immunol.* 163:3890–3897.

38. Larsen, C.P., R.M. Steinman, M. Witmer-Pack, D.F. Hankins, P.J. Morris, and J.M. Austyn. 1990. Migration and maturation of Langerhans cells in skin transplants and explants. *J. Exp. Med.* 172:1483–1493.

39. Belkaid, Y., H. Jouin, and G. Milon. 1996. A method to recover, enumerate and identify lymphomyeloid cells present in an inflammatory dermal site: a study in laboratory mice. *J. Immunol. Methods.* 199:5–25.

40. Belkaid, Y., S. Kamhawi, G. Modi, J. Valenzuela, N. Noben-Trauth, E. Rowton, J. Ribeiro, and D.L. Sacks. 1998. Development of a natural model of cutaneous leishmaniasis: powerful effects of vector saliva and saliva preexposure on the long-term outcome of *Leishmania major* infection in the mouse ear dermis. *J. Exp. Med.* 188:1941–1953.

41. Larsen, C.P., S.C. Ritchie, R. Hendrix, P.S. Linsley, K.S. Hathcock, R.J. Hodes, R.P. Lowry, and T.C. Pearson. 1994. Regulation of immunostimulatory function and costimulatory molecule (B7-1 and B7-2) expression on murine dendritic cells. *J. Immunol.* 152:5208–5219.

42. Hill, S., A.J. Edwards, I. Kimber, and S.C. Knight. 1990. Systemic migration of dendritic cells during contact sensitization. *Immunology.* 71:277–281.

43. Macatonia, S.E., A.J. Edwards, and S.C. Knight. 1986. Dendritic cells and the initiation of contact sensitivity to fluorescein isothiocyanate. *Immunology.* 59:509–514.

44. Macatonia, S.E., S.C. Knight, A.J. Edwards, S. Griffiths, and P. Fryer. 1987. Localization of antigen on lymph node dendritic cells after exposure to the contact sensitizer fluorescein isothiocyanate. Functional and morphological studies. *J. Exp. Med.* 166:1654–1667.

45. Thomas, W.R., A.J. Edwards, M.C. Watkins, and G.L. Asherson. 1980. Distribution of immunogenic cells after painting with the contact sensitizers fluorescein isothiocyanate and oxazolone. Different sensitizers form immunogenic complexes with different cell populations. *Immunology.* 39:21–27.

46. Leenen, P.J., K. Radosevic, J.S. Voerman, B. Salomon, N. van Rooijen, D. Klatzmann, and W. van Ewijk. 1998. Heterogeneity of mouse spleen dendritic cells: in vivo phagocytic activity, expression of macrophage markers, and subpopulation turnover. *J. Immunol.* 160:2166–2173.

47. Miyazaki, H., and T. Osawa. 1983. Accessory functions and mutual cooperation of murine macrophages and dendritic cells. *Eur. J. Immunol.* 13:984–989.

48. Inaba, K., W.J. Swiggard, R.M. Steinman, N. Romani, and G. Schuler. 1998. Enrichment of dendritic cells by plastic adherence and EA rosetting. *In* Current Protocols in Immunology. J.E. Coligan, A.M. Kruisbeek, D.H. Margulies, E.M. Shevach, and W. Strober, editors. John Wiley & Sons, New York. 3.7.1–3.7.15.

49. Randolph, G.J., K. Inaba, D.F. Robbiani, R.M. Steinman, and W.A. Muller. 1999. Differentiation of phagocytic monocytes into lymph node dendritic cells in vivo. *Immunity.* 11:753–761.

50. Sato, K., Y. Imai, and T. Irimura. 1998. Contribution of dermal macrophage trafficking in the sensitization phase of contact hypersensitivity. *J. Immunol.* 161:6835–6844.

51. De Smedt, T., B. Pajak, E. Muraille, L. Lespagnard, E. Heinen, P. De Baetselier, J. Urbain, O. Leo, and M. Moser. 1996. Regulation of dendritic cell numbers and maturation by lipopolysaccharide in vivo. *J. Exp. Med.* 184:1413–1424.

52. Mattner, F., J. Magram, J. Ferrante, P. Launois, K. Di Padova, R. Behin, M.K. Gately, J.A. Louis, and G. Alber. 1996. Genetically resistant mice lacking interleukin-12 are susceptible to infection with *Leishmania major* and mount a polarized Th2 cell response. *Eur. J. Immunol.* 26:1553–1559.

53. Leal, L.M., D.W. Moss, R. Kuhn, W. Muller, and F.Y. Liew. 1993. Interleukin-4 transgenic mice of resistant background are susceptible to *Leishmania major* infection. *Eur. J. Immunol.* 23:566–569.

54. Grouard, G., I. Durand, L. Filgueira, J. Banchereau, and Y.J. Liu. 1996. Dendritic cells capable of stimulating T cells in germinal centres. *Nature.* 384:364–367.

55. Ngo, V.N., H. Korner, M.D. Gunn, K.N. Schmidt, D.S. Riminton, M.D. Cooper, J.L. Browning, J.D. Sedgwick, and J.G. Cyster. 1999. Lymphotoxin α/β and tumor necrosis factor are required for stromal cell expression of homing chemokines in B and T cell areas of the spleen. *J. Exp. Med.* 189:403–412.

56. Blanpain, C., I. Migeotte, B. Lee, J. Vakili, B.J. Doranz, C. Govaerts, G. Vassart, R.W. Doms, and M. Parmentier. 1999. CCR5 binds multiple CC-chemokines: MCP-3 acts as a natural antagonist. *Blood.* 94:1899–1905.

57. Imai, T., T. Yoshida, M. Baba, M. Nishimura, M. Kakizaki, and O. Yoshie. 1996. Molecular cloning of a novel T cell-directed CC chemokine expressed in thymus by signal sequence trap using Epstein-Barr virus vector. *J. Biol. Chem.* 271:21514–21521.

58. Anjuere, F., G. Martinez del Hoyo, P. Martin, and C. Ardavin. 2000. Langerhans cells acquire a CD8+ dendritic cell phenotype on maturation by CD40 ligation. *J. Leukoc. Biol.* 67:206–209.

59. Gu, L., S. Tseng, R.M. Horner, C. Tam, M. Loda, and B.J. Rollins. 2000. Control of T_H2 polarization by the chemokine monocyte chemoattractant protein-1. *Nature.* 404:407–411.

60. Mohrs, M., B. Ledermann, G. Kohler, A. Dorfmuller, A. Gessner, and F. Brombacher. 1999. Differences between IL-4- and IL-4 receptor alpha-deficient mice in chronic leishmaniasis reveal a protective role for IL-13 receptor signaling. *J. Immunol.* 162:7302–7308.

61. Doetschman, T. 1999. Interpretation of phenotype in genetically engineered mice. *Lab. Anim. Sci.* 49:137–143.

62. Erickson, R.P. 1996. Mouse models of human genetic disease: which mouse is more like a man? *Bioessays.* 18:993–998.

63. Noben-Trauth, N., W.E. Paul, and D.L. Sacks. 1999. IL-4- and IL-4 receptor-deficient BALB/c mice reveal differences in susceptibility to *Leishmania major* parasite substrains. *J. Immunol.* 162:6132–6140.

64. Ingulli, E., A. Mondino, A. Khoruts, and M.K. Jenkins. 1997. In vivo detection of dendritic cell antigen presentation

to CD4^{+} T cells. *J. Exp. Med.* 185:2133–2141.

65. Himmelrich, H., C. Parra-Lopez, F. Tacchini-Cottier, J.A. Louis, and P. Launois. 1998. The IL-4 rapidly produced in BALB/c mice after infection with *Leishmania major* down-regulates IL-12 receptor beta 2-chain expression on CD4+ T cells resulting in a state of unresponsiveness to IL-12. *J. Immunol.* 161:6156–6163.

66. Launois, P., T. Ohteki, K. Swihart, H.R. MacDonald, and J.A. Louis. 1995. In susceptible mice, *Leishmania major* induce very rapid interleukin-4 production by CD4+ T cells which are NK1.1. *Eur. J. Immunol.* 25:3298–3307.

67. Mitchison, N.A., D. Schuhbauer, and B. Muller. 1999. Natural and induced regulation of Th1/Th2 balance. *Springer Semin. Immunopathol.* 21:199–210.

68. Rossi-Bergmann, B., I. Muller, and E.B. Godinho. 1993. TH1 and TH2 T-cell subsets are differentially activated by macrophages and B cells in murine leishmaniasis. *Infect. Immun.* 61:2266–2269.

69. Randolph, D.A., G. Huang, C.J. Carruthers, L.E. Bromley, and D.D. Chaplin. 1999. The role of CCR7 in TH1 and TH2 cell localization and delivery of B cell help in vivo. *Science.* 286:2159–2162.